Mechanism of Inorganic Phosphate Interaction with Phosphate Binding Protein from *Escherichia coli*†

Martin Brune,‡ Jackie L. Hunter,‡ Steven A. Howell,‡ Stephen R. Martin,‡ Theodore L. Hazlett,§ John E. T. Corrie,‡ and Martin R. Webb*,‡

National Institute for Medical Research, Mill Hill, London NW7 1AA, U.K., and Laboratory for Fluorescence Dynamics, University of Illinois at Urbana-Champaign, Urbana, Illinois 61801

Received February 23, 1998; Revised Manuscript Received May 12, 1998

ABSTRACT: The mechanism of P_i interaction with phosphate binding protein of *Escherichia coli* has been investigated using the A197C mutant protein labeled with a coumarin fluorophore (MDCC−PBP), which gives a fluorescence change on binding P_i. A pure preparation of MDCC−PBP was obtained, in which the only significant inhomogeneity is the presence of equal amounts of two diastereoisomers due to the chiral center formed on reaction of the cysteine with the maleimide. These diastereoisomers could not be separated, but P_i binding data suggest that they differ in affinity and fluorescence change. When P_i binds to MDCC−PBP, the fluorescence quantum yield increases 8-fold and the fluorescence intensity at 465 nm increases 13-fold. The kinetics of P_i binding show saturation of the rate at high P_i concentrations, and this together with other information suggests a two-step mechanism with the fluorescence change after binding, concomitant with a conformational change of the protein that closes the cleft containing the P_i binding site. Cleft closure has a rate constant of 317 s^{-1} (pH 7.0, 5 °C), and opening has a rate constant of 4.5 s^{-1}. The fluorescence increase is likely to arise from a change in the hydrophobic environment during this closure as the steady state fluorescence emission (λ_{max} and intensity) on P_i binding is mimicked by the addition of ethanol to aqueous solutions of an MDCC−thiol adduct. Fluorescence lifetimes in the absence and presence of P_i were 0.3 and 2.4 ns, respectively, consistent with the change in quantum yield. The rotational correlation time of the coumarin increases only 2-fold from 15 to 26 ns on binding P_i as measured by time-resolved polarization, consistent with the main rotation being determined by the protein even in the open conformation, but with greater local motion. Circular dichroism of the coumarin induced by the protein is weak in the absence of P_i and increases strongly upon saturation by P_i. These data are also consistent with an open to closed conformational model.

Phosphate binding protein (PBP)[1] of *Escherichia coli* is a member of a class of proteins that are produced and transported to the periplasm in response to the absence (starvation) of certain essential nutrients. PBP is produced under conditions of low inorganic phosphate (P_i) concentrations and scavenges in the periplasm for P_i, which it then transfers to a membrane protein for transport into the cytoplasm. Such periplasmic binding proteins have been identified for anions (e.g., sulfate), sugars (e.g., arabinose), and amino acids (e.g., leucine). They have very little sequence similarity, but the overall fold is rather similar for members of the class for which structures have been determined; there are two hinged domains with a binding cleft between them (*1*), and the binding mechanism has been described as the Venus flytrap model with a large relative rotation of the domains to enclose the ligand (*2*).

The development of the phosphate binding protein from *E. coli* as a probe for P_i has been reported (*3*). A single cysteine, introduced into the protein at position 197 by oligonucleotide-directed mutagenesis, is selectively labeled with a fluorophore, *N*-[2-(1-maleimidyl)ethyl]-7-(diethylamino)coumarin-3-carboxamide (MDCC). The resultant labeled protein (MDCC−PBP) as then reported gives an ∼7-fold increase in fluorescence at 465 nm when the P_i level is saturating. The binding of P_i to this probe is rapid (1.36×10^8 M^{-1} s^{-1} at 22 °C) and tight ($K_d \sim 0.1$ μM) so that the probe is sensitive in the nanomolar range of P_i. MDCC−PBP has been used to investigate the kinetics and role of P_i release in a number of systems that involve ATP or GTP hydrolysis (*3*−*7*). Because of the tight and rapid binding of P_i to MDCC−PBP, the kinetics and size of the observed fluorescence change correspond to the rate and stoichiometry of P_i release from the relevant phosphatase.

† This work was supported by the Medical Research Council, U.K., and by NIH Grant RR03155 to the Laboratory for Fluorescence Dynamics.

* To whom correspondence should be addressed. Telephone: (44) 181 959 3666. Fax: (44) 181 906 4477. E-mail: m-webb@nimr.mrc.ac.uk.

‡ National Institute for Medical Research.

§ University of Illinois at Urbana-Champaign.

[1] Abbreviations: PBP, phosphate binding protein; MDCC, *N*-[2-(1-maleimidyl)ethyl]-7-(diethylamino)coumarin-3-carboxamide; IDCC, *N*-[2-(iodoacetamido)ethyl]-7-(diethylamino)coumarin-3-carboxamide; MDCC−PBP, A197C mutant of PBP labeled with MDCC; MDCC−MES, product of reacting MDCC with 2-mercaptoethanesulfonate; MEG, 7-methylguanosine; MDCC−DTT, product of reacting MDCC with dithiothreitol; PNPase, purine nucleoside phosphorylase; PDRM, phosphodeoxyribomutase; Coumarin 314, ethyl 2,3,6,7-tetrahydro-11-oxo-1*H*,5*H*,11*H*-[1]benzopyrano[6,7,8-*i*,*j*]quinazoline-10-carboxylate; LC−MS, liquid chromatography−mass spectrometry; DTNB, 5,5′-dithiobis(2-nitrobenzoic acid).

S0006-2960(98)00427-9 CCC: $15.00
Published on Web 07/01/1998

The development of this labeled PBP provided a route for investigating the mechanism of P_i binding to PBP; however, to use MDCC−PBP for this purpose, it was essential to have a preparation as homogeneous as possible, and the steps taken to achieve this are described. We have improved the efficiency of labeling and performance of the MDCC−PBP probe by using an enhanced "P_i mop" to remove contaminant P_i (A. E. Nixon, J. L. Hunter, and M. R. Webb, unpublished result). This mop involves chemical removal of P_i by a coupled enzyme system, purine nucleoside phosphorylase (PNPase) and phosphodeoxyribomutase (PDRM) with 7-methylguanosine (MEG) as the substrate, which results in P_i being sequestered in a stable form as ribose 5-phosphate. Side products of the labeling have been identified as being due to labeling at a specific lysine and to hydrolysis, probably at the succinimide ring (eq 1, where R represents the coumarin−ethylene moiety and R′ the protein).

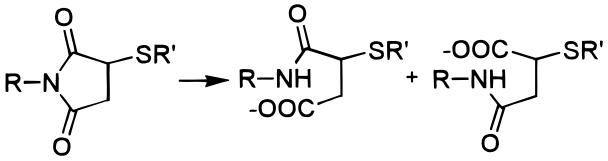

(1)

In addition, the MDCC−PBP preparation contains a fraction that is not responsive to P_i, although it has the same mass and tryptic digestion pattern as the responsive protein and so has the same polypeptide as the responsive form. Changes in labeling and purification protocols have almost eliminated these side products, allowing the preparation of well-defined P_i-bound and P_i-free PBP for studying conformational differences and the kinetics of interconversion. The P_i-responsive form of MDCC−PBP consists of equal amounts of two diastereoisomers, produced as a result of the labeling reaction (eq 2), probably due to the maleimide ring presenting one face to the cysteine but with either electrophilic carbon equally accessible and reactive to the cysteine.

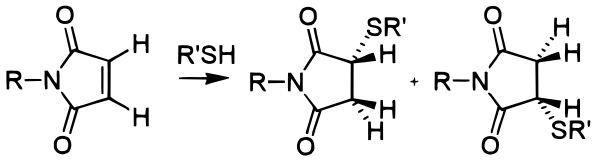

(2)

R = *N*-[2-(7-diethylaminocoumarin-3-carboxyamido)ethyl]
R'SH = A197C mutant of PBP

The mixture of diastereoisomers has not so far proved to be separable but gives an ∼13-fold increase in fluorescence at 465 nm on saturation with P_i.

This highly purified MDCC−PBP was used to investigate the mechanism of P_i binding to PBP, using kinetic and spectroscopic measurements to probe the conformational change associated with P_i binding. It is likely that the same general mechanism exists in other periplasmic ligand binding proteins, but the existence of the highly purified fluorescently labeled PBP has allowed a number of approaches for understanding the mechanism that would not be possible currently with other members of this class of proteins. In doing this, we have also investigated the factors that produce the associated fluorescence change. The following paper (*8*) describes the high-resolution crystal structure of MDCC−PBP, which allows us to analyze the high fluorescence state and other spectroscopic properties in terms of the environment of the coumarin on the protein.

EXPERIMENTAL PROCEDURES

Materials. PDRM was prepared from an *E. coli* expression system (A. E. Nixon, J. L. Hunter, and M. R. Webb, unpublished result). Glycerokinase from *E. coli* and "bacterial" PNPase were from Sigma and were stored as solutions frozen at −80 °C at 7 mg mL^{-1} and 500 units mL^{-1}, respectively. Other substrates and cofactors were from Sigma.

MDCC−PBP was prepared as described by Brune et al. (*3*) with the following changes. The expression of PBP by the *E. coli* is critically dependent on growth conditions, and the following conditions consistently give ∼500 mg of A197C protein after purification from a 4 L culture. Vigorous shaking of the culture medium was used throughout to ensure good aeration. LB medium (10 mL) containing 12.5 mg L^{-1} tetracycline was inoculated with *E. coli* ANCC75 harboring plasmid pSN5182/7 with the mutated *pho*S gene. After 6 h at 37 °C, this culture was diluted to 100 mL with the same medium and grown for 16 h at 37 °C. For each of eight 500 mL final cultures, 10 mL of the 16 h culture was diluted into 500 mL of high-phosphate TG plus medium with supplements (*3*) containing 12.5 mg L^{-1} tetracycline. The culture was incubated at 37 °C for ∼6 h until the optical density at 600 nm was 2.0 cm^{-1}. Cells were pelleted by centrifugation at 3000 rpm at room temperature for 30 min in autoclaved centrifuge bottles and resuspended in 500 mL of TG plus containing the same supplements except 64 μM KH_2PO_4 was used. Cells were grown for another 16 h and then harvested by centrifugation at room temperature at 4000 rpm for 25 min.

PBP was released from the cells' periplasm by osmotic shock (*9*). The cell supernatant was discarded, and pellets were resuspended in a total of 650 mL of 10 mM Tris·HCl (pH 7.6) and 30 mM NaCl at room temperature. The suspension was pooled into one 1 L centrifuge bottle and spun as above. The supernatant was discarded, and the cells were resuspended in 350 mL of the same buffer. After centrifugation as above, the supernatant was removed and the pellet weighed (typically, 15 g from a 4 L culture). Cells were then resuspended in 100 mL of 33 mM Tris·HCl (pH 7.6) at 25 °C and transferred to one 250 mL centrifuge bottle containing a magnetic stir bar.

One hundred milliliters of 40% sucrose, 0.1 mM EDTA, and 33 mM Tris·HCl (pH 7.6) at 25 °C was added quickly while the solution was stirred rapidly on a magnetic stirrer. After the mixture was stirred for 10 min at 25 °C, cells were spun at 10 000 rpm for 20 min at 4 °C. After the supernatant was discarded, the cells were resuspended rapidly in 200 mL of ice cold 0.5 mM $MgCl_2$ to break outer membranes and release PBP. After the mixture was stirred rapidly for 15 min in an ice bath, the cells were spun at 10 000 rpm for 10 min at 4 °C.

The supernatant (typically, 200 mL) was made 10 mM in Tris·HCl (pH 7.6) and applied to a Q-Sepharose column (100 mL), equilibrated with 10 mM Tris·HCl (pH 7.6) and 1 mM $MgCl_2$. After loading, the column was washed with 1 column volume of equilibration buffer, and then a 1 L linear gradient of 0 to 200 mM NaCl in the same buffer was

applied. PBP was the major protein present and was pooled and concentrated in an Amicon pressure concentrator. The final protein solution was stored in small aliquots at −80 °C. Protein concentrations were based on absorbance at 280 nm assuming an extinction coefficient ($E^{1\%}$ at 280 nm) of 17.8 cm^{-1}, which is based on the theoretical value (*10*).

The much greater reactivity of the thiol in the P_i-free form of PBP (see below) led us to change the labeling conditions, using the P_i mop to maintain very low P_i concentrations during the reaction of MDCC (*11*) with the A197C PBP and so to allow more rapid and complete labeling. Previously, the labeling efficiency was variable, typically, ∼50%. Under the conditions described here, >95% labeling was achieved. The A197C PBP mutant (28 mg) was labeled for 30 min at 20 °C in a solution [8 mL of 20 mM Tris·HCl (pH 8.1)] containing 100 μM PBP, 150 μM MDCC, 200 μM MEG, 0.2 unit mL^{-1} PNPase, 5 μM $MnCl_2$, 1 μM glucose 1,6-bisphosphate, and 1 μg mL^{-1} PDRM, with end-over-end mixing and protection from light. The protein had low-molecular weight species removed by P4 gel (Bio-Rad) filtration (*3*) and was then loaded onto a 10 mL Q-Sepharose column (Pharmacia), equilibrated with 10 mM Tris·HCl (pH 8.0). After being washed, the protein was eluted with a 400 mL linear gradient from 0 to 50 mM NaCl in this buffer. This procedure gave typically a 50% yield of the main P_i-responsive protein after concentration, and this was stored at −80 °C.

MDCC−PBP (7 mg) from Q-Sepharose was further purified on a Mono Q column (5 cm × 0.5 cm, Pharmacia), eluting at 1 mL min^{-1} using a 30 min linear gradient from 0 to 30 mM NaCl in 10 mM Tris·HCl (pH 8.0) and 100 μM P_i. This resulted in two PBP peaks, P_i-responsive and nonresponsive protein. Unlabeled PBP coelutes with the major labeled peak of P_i-responsive protein on this column; hence, it is important to have no unlabeled protein present during this chromatography. Each protein was concentrated to 0.5 mL using a Centricon membrane (Amicon), and then treated for 1 h at 20 °C with the enhanced P_i mop, which consisted of 1 unit mL^{-1} PNPase, 600 μM MEG, 20 μM $MnCl_2$, 1 μM glucose 1,6-bisphosphate, and 2 μg mL^{-1} PDRM. The MDCC−PBP was then diluted to 2.5 mL with 10 mM Tris·HCl (pH 8.0) and concentrated to ∼1 mM. The dilution and concentration steps were repeated a total of three times to remove low-molecular weight components of the P_i mop.

Tryptic Digestion and HPLC. Fifty microliters of 400 μM MDCC−PBP was made 6 M in guanidinium chloride and then diluted 6-fold. The solution was made 20 mM in $CaCl_2$ and 50 mM in NH_4HCO_3, and 35 μg of trypsin (Worthington) was added. The solution was incubated at 37 °C overnight before HPLC analysis of aliquots (20 μL) on a reverse phase silica column (Vydac, Protein and Peptide C18, 25 cm × 0.4 cm). The 60 min gradient was 1% (v/v) acetonitrile and 0.06% trifluoroacetic acid in water to 66% acetonitrile and 0.058% trifluoroacetic acid, at 1 mL min^{-1}, and elution was monitored at 215 nm.

Absorbance and Fluorescence Measurements. Absorbance spectra were obtained on a Beckman DU70 spectrophotometer. Fluorescence measurements were obtained on a Perkin-Elmer LS50B fluorimeter with a xenon lamp. For time-resolved measurements, slit widths were 2.5 nm for excitation and 5 nm for emission. Stopped flow experiments were carried out in a HiTech SF61MX apparatus, with a mercury lamp and HiTech IS-2 software. There were a monochromator and 5 nm slits for the excitation light and a 455 nm cutoff filter for the emission.

Mass Spectrometry. Electrospray mass spectra were acquired on a VG Platform using nitrogen as the nebulizer gas. Protein analysis of 50 pmol samples was achieved by "on-line" trapping, using a 100 mm × 0.25 mm PEEK column packed with 10 μm Poros R2 medium (Perseptive Biosystems Inc.), as described earlier (*12*). Microbore LC−MS was carried out by coupling an Applied Biosystems 120A HPLC to the mass spectrometer using 50 μm inside diameter fused silica tubing. A low-dead volume tee-piece (Valco ZV1T) was inserted just before the mass spectrometer and set to give a split of 1:4 (mass spectrometer:collection). Chromatography was performed using a Vydac C18 250 mm × 1 mm column (no. 218TP51) at a flow rate of 50 μL min^{-1} and a gradient of 1% min^{-1} using the same buffer system as described earlier and monitoring at 215 nm.

Analytical Ultracentrifugation. This was carried out in a Beckman XLA analytical ultracentrifuge at 20 °C by monitoring absorbance at 430 nm through the 1.2 cm path length. MDCC−PBP at 4.4 and 13.3 μM in 10 mM PIPES (pH 7.0) and 1 mM $MgCl_2$ with excess P_i or with the P_i mop was spun at 15 000 and then 20 000 rpm for sufficient time at each speed for equilibrium to be reached. Finally, each sample was centrifuged at 40 000 rpm for 2 h to deplete the meniscus and hence obtain baseline absorbance. Data were analyzed using the Beckman Origin software program by fitting to a single ideal species with a varying molecular weight. The density of the buffer solution was assumed to be 0.998 g mL^{-1}, and the partial specific volume of the protein was calculated from its amino acid sequence to be 0.735 mL g^{-1}.

Circular Dichroism. CD spectra were recorded on a Jasco J-600 spectropolarimeter at 20 °C, using 1 (far-UV) or 10 mm (near-UV−visible) fused silica cuvettes.

Time-Resolved Fluorescence. Fluorescence lifetime and dynamic polarization data were recorded on a multifrequency cross-correlation phase and modulation fluorometer (ISS Inc., Champaign, IL). Sample excitation was at 350 nm from the output of a Nd:YAG-pumped DCM dye laser (Coherent, Palo Alto, CA) tuned to 700 nm and frequency-doubled to 350 nm. The sample emission was observed through a Schott KV 399 long pass filter to eliminate scattered excitation light and transmit fluorescence (>375 nm). POPOP [1,4-bis(5-phenyloxazol-2-yl)benzene] was used as the lifetime standard (1.35 ns). To correct for polarization artifacts in the fluorescence lifetime data, data were collected with the excitation beam polarized at 0° relative to the laboratory plane, and the emission was viewed through a polarizer set to 54.7° (*13*). Unless otherwise stated, samples were held at 20 °C during data acquisition. Fluorescence lifetime and dynamic polarization data were analyzed using Globals Unlimited (Laboratory for Fluorescence Dynamics, University of Illinois, Urbana, IL) and were fit to standard multiexponential decay models. Further information on multifrequency phase and modulation fluorometry can be found in the literature (*14*−*17*).

RESULTS

The main spectroscopic and kinetic experiments were aimed at understanding the mechanism by which P_i binds to PBP. An essential part of obtaining and analyzing the mechanistic data was understanding the chemistry of labeling and preparing the pure protein. So we first show evidence that a pair of diastereoisomers are present. We then describe the identification of other species formed on labeling PBP with MDCC and the steps for producing the highly purified P_i-responsive protein in which the diastereoisomers are the only significant inhomogeneity.

Diastereoisomers. MDCC−PBP was subjected to tryptic digestion followed by reverse phase HPLC of the digest. Apart from peptide peaks also identified in the tryptic digest of wild type PBP, there were two peaks of equal size that appeared as a closely eluting doublet and were yellow and fluorescent. Electrospray mass spectrometry showed that both had the same mass, which corresponded to that predicted for the tryptic peptide (LPGAIGYVEYCYAK) with the cysteine labeled with MDCC. We were unable to separate the two labeled proteins containing these peptides, and conditions where the ratio of the two species deviated from 1 were not found. It is probable that this doublet corresponds to the two diastereoisomers (eq 2).

To investigate this further, we used IDCC, the iodoacetamide analogue of MDCC (*11*) to label the cysteine of A197C PBP. With IDCC, the distance of the coumarin from the thiol is the same number of bonds as that with MDCC; however, the reaction of IDCC with the thiol does not produce a new chiral center, so only one species should be present. Labeling with IDCC was significantly slower than with MDCC, and <50% of the protein was labeled after 7 h. The fluorescence of the labeled protein was almost insensitive to P_i, showing a <5% decrease upon saturation with P_i. Tryptic digestion of the labeled protein now produced only one HPLC peak in a position similar to that of the MDCC−PBP doublet. This peak had the mass expected for the IDCC-labeled peptide, supporting the hypothesis that the doublet from MDCC−PBP is due to diastereoisomers.

Hydrolysis of the Labeled Product. On extended incubation of the MDCC-labeled protein at pH ≥8 and at elevated temperatures, the labeled peptide doublet decreased in intensity in the HPLC profile of the tryptic digest and three new peaks appeared. All three new peaks had a mass 18 Da higher than the those of the labeled peptides. It seems likely that there is a base-catalyzed hydrolysis of the succinimide ring as in eq 1, potentially giving four different species. The relative heights of the three observed peaks suggest that there are two doublets present in which two peaks overlap. After incubation of MDCC−PBP for 17 h at 37 °C, there was negligible hydrolysis at pH 7.0, ∼50% at pH 8.0, and 100% at pH 9.0. The kinetics of the hydrolysis were followed in a test reaction using the MDCC−MES adduct, which hydrolyzed at 0.9 h^{-1} at pH 10 and 20 °C, as monitored by anion exchange HPLC. Thus, hydrolysis is unlikely to be a problem under the normal conditions of preparation or use of MDCC−PBP.

Other Species. Two other species could be separated by ion exchange chromatography from the main P_i-responsive protein, a doubly labeled form and a form whose fluorescence is not responsive to P_i binding. Electrospray mass spectrometry showed that the responsive PBP has a mass of 34 838 (±3) Da which is consistent with the predicted mass (34 836.5 Da) for MDCC−PBP. With some labeling conditions, there was a species present that had a mass of 35 229 (±2) Da, 392 Da greater than that of MDCC−PBP. HPLC−mass spectrometry of the tryptic digest revealed a minor peptide consistent with a small amount of second labeling by MDCC at K175, which prevents tryptic cleavage at this position. Doubly labeled protein should have a mass 383 Da greater than that of the singly labeled species. However, partial hydrolysis of the two succinimides that occurs under basic conditions, as in eq 1, results in two different masses, 18 Da apart. Hydrolysis of the N-linked succinimide is probably faster than that of the S-linked species because of the greater electronegativity of the nitrogen. The hydrolyzed and unhydrolyzed species would not be resolved on the electrospray mass spectrometer, so an average mass is observed. The amount of doubly labeled species was 7.5% of the total MDCC−PBP for the 4 h labeling conditions as described (*3*) but was negligible for the conditions described here. This calculation assumes that the relative size of peaks in the mass spectrum is proportional to the relative amounts of protein, and although this assumption may not be fully valid, it does give an indication of the decrease in extent of double labeling with decreasing labeling time and excess of MDCC.

In the presence of P_i (but not in its absence), a further MDCC−PBP species could be isolated by ion exchange chromatography that had the same mass and tryptic digest pattern, but showed a <2-fold increase in fluorescence on binding P_i. All this increase can be explained by the presence of a small amount of responsive MDCC−PBP, so this species' fluorescence is probably not sensitive to P_i. The P_i-responsive MDCC−PBP from the first protein peak of Mono Q purification was incubated for 70 h at 20 °C in 10 mM Tris·HCl (pH 7.6) to determine the extent of conversion to nonresponsive protein, and the solution was analyzed by chromatography on Mono Q. In the presence of P_i, 1.5% was converted; in the presence of the P_i mop, 7% was converted. Thus, the P_i-free protein can be converted to the nonresponsive form, and P_i binding inhibits this conversion. The nonresponsive protein is presumably a different conformational state, and this point is addressed in the Discussion.

Subsequent data were collected with the responsive protein, purified by the procedures described in this paper. Except where identified, the term MDCC−PBP refers to this responsive protein.

Absence of Oligomerization. Equilibrium analytical centrifugation was performed at two different concentrations and two speeds, in the presence of P_i or the P_i mop. In all cases, the data were consistent with a single species with a molecular weight within 9% of that of the monomer.

Steady State Fluorescence. Fluorescence spectra of the P_i-responsive MDCC−PBP (Figure 1) showed a 13-fold enhancement of fluorescence at 465 nm. The titration curve with P_i is similar to that described by Brune et al. (*3*), showing ∼75% activity assuming a single population (Figure 2). However, it is also possible to interpret the titration curves as arising from 100% active protein, with 50% giving a large fluorescence change and 50% giving a smaller

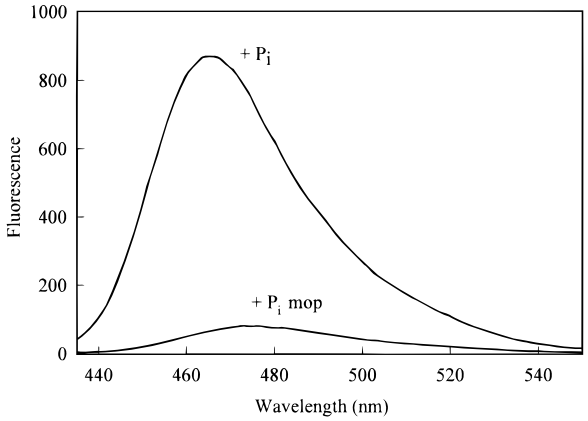

FIGURE 1: Fluorescence emission spectra of MDCC−PBP in the presence and absence of P_i. The solution was 7 μM MDCC−PBP in 10 mM PIPES (pH 7.0) at 21 °C. Fifteen micromolar P_i or the P_i mop (300 μM MEG, 2 units mL^{-1} PNPase) was also present. The excitation wavelength was 430 nm.

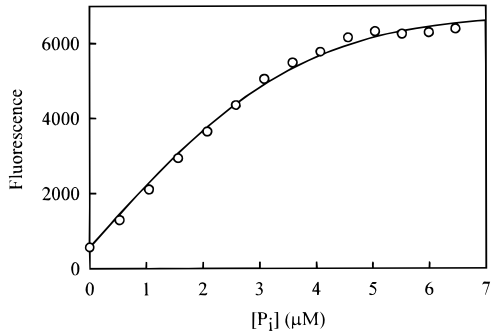

FIGURE 2: Titration of P_i to MDCC−PBP. The solution at 20 °C contained 5.6 μM MDCC−PBP and 10 mM PIPES (pH 7.0). Aliquots of P_i were added, and the fluorescence intensity was corrected for the small dilution. [P_i] was corrected for a small amount of P_i present in the initial solution, determined using the enhanced mop (300 μM MEG, 1 unit mL^{-1} PNPase, 1 μM glucose 1,6-bisphosphate, 5 μM $MnCl_2$, and 2.5 μg mL^{-1} PDRM). The theoretical curve is for two equal populations of protein. One has a K_d of 0.05 μM and a 20-fold increase in fluorescence on adding P_i; the other has a K_d of 0.4 μM and a 4.7-fold increase in fluorescence. Both populations had the same P_i-free fluorescence. However, a range of values for these variables gave similar curves when the ratio of K_d values was ~10 and the tighter binding protein had a fluorescence increase of 12−20-fold.

fluorescence change with weaker binding. This latter suggestion is consistent with the presence of the two diastereoisomers and will be discussed further below.

Kinetics of P_i Binding and Release. The second-order rate constant for P_i binding to MDCC−PBP had been determined previously at 20 °C using rapid mixing at several concentrations of P_i (*3*). At that temperature and high P_i concentrations, the observed rates were too fast to determine whether the rate of binding was a hyperbolic function of P_i concentration or whether the observed rates became limited by the stopped flow instrument. To overcome this problem, we repeated the measurements at 5 °C and showed that there is saturation of the observed rate at high P_i concentrations (Figure 3). The hyperbolic shape is consistent with a two-step mechanism (eq 3).

$$\text{MDCC−PBP} + P_i \overset{1}{\rightleftharpoons} \text{MDCC−PBP}\cdot P_i \overset{2}{\rightleftharpoons} \text{MDCC−PBP*}\cdot P_i \quad (3)$$

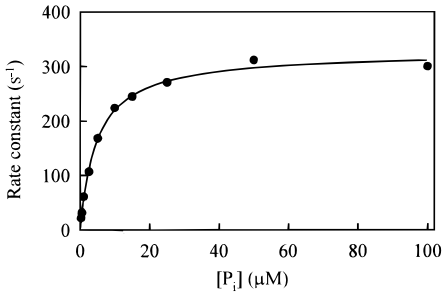

FIGURE 3: Dependence of the kinetics of P_i binding to MDCC−PBP on [P_i]. MDCC−PBP (0.1 μM) (mixing chamber concentrations), containing 0.1 unit mL^{-1} PNPase and 20 μM MEG, was mixed with P_i in 10 mM PIPES buffer (pH 7.0) at 5 °C. The increase in fluorescence was fitted to a single exponential, and at least three measurements were averaged. The best-fit line is for a two-step process (eq 3), where step 1 is rapid, so that the observed rate constant equals $k_2/(1 + [P_i]K_1) + k_{-2}$ where $1/K_1 = 4.9$ μM and $k_2 + k_{-2} = 322$ s^{-1}. The intercept was not accurate enough to define k_{-2}.

We define the equilibrium constant and the forward and reverse rate constants of step *i* as K_i, k_i, and k_{-i}, respectively. The asterisk indicates a different conformational state of the complex, whose formation (step 2) is likely to generate all the increased fluorescence. The product of step 1 would have the same low fluorescence as unliganded MDCC−PBP. It is likely that step 1 corresponds to the formation of a collision complex and step 2 to the closing of the cleft that contains the P_i binding site (*18*), thereby changing the environment of the fluorophore that is attached to the cysteine located at the lip of the cleft. Physical measurements will be discussed later in terms of this model.

The reverse reaction was also measured at 5 °C by displacing P_i from the MDCC−PBP·P_i complex using a large excess of wild type PBP as previously described (*3*). The observed rate constant was 4.8 s^{-1} (data not shown), interpreted as k_{-2} in the Discussion. P_i release kinetics were measured at different levels of saturation by P_i and 2.5 μM MDCC−PBP to obtain either one or both P_i-bound diastereoisomers. In all cases, the fluorescence fit well a single exponential, so there was no evidence for the two diastereoisomers exhibiting different release kinetics. The question of how the diastereoisomers may differ is addressed in the Discussion. The release kinetics were also measured for wild type PBP (3.5 s^{-1}) and the nonresponsive PBP (50−60 s^{-1}), in each case by rapid mixing with excess unliganded MDCC−PBP.

Thiol Accessibility. Because of the large change in fluorescence on binding of P_i to MDCC−PBP and because the kinetics of P_i binding suggested a conformational change associated with P_i binding, it seemed possible that the accessibility of Cys197 would change on P_i binding. To test this, the reaction of DTNB with the thiol on the A197C mutant was followed using the change in absorbance under pseudo-first-order conditions (Figure 4). The rate constant is 1.9×10^{-4} s^{-1} in the presence of P_i and 0.014 s^{-1} (70-fold faster) in the absence of P_i. Structural implications of this result will be considered in the Discussion.

Hydrophobic Environment. The effect on fluorescence of changing the hydrophobicity of the coumarin environment was measured for MDCC−DTT by titrating the proportion of ethanol in the solvent. Figure 5 shows that, as the proportion of ethanol in the solvent increases, the fluores-

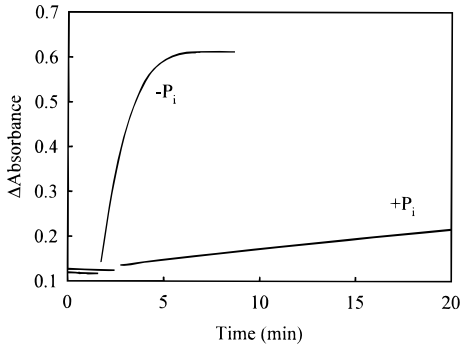

FIGURE 4: Kinetics of DTNB reaction with the cysteine of A197C PBP in the presence and absence of P_i. The reaction mixture was 1 mM DTNB and 27 μM PBP in 100 mM Tris·HCl (pH 8.0) at 21 °C. P_i at 270 μM or the enhanced mop (300 μM MEG, 1 unit mL^{-1} PNPase, 1 μM glucose 1,6-bisphosphate, 5 μM $MnCl_2$, and 2.5 μg mL^{-1} PDRM) was also present. The reactions were followed to completion by absorbance at 412 nm, and the whole data sets were used to fit to pseudo-first-order reaction kinetics.

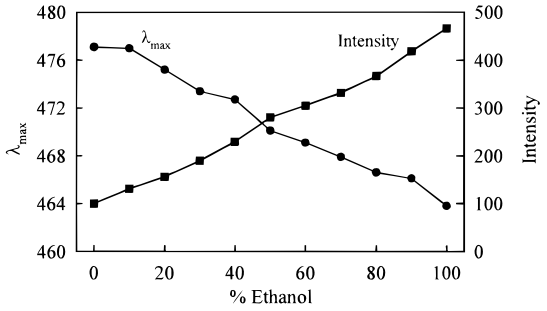

FIGURE 5: Effect of ethanol on MDCC−DTT adduct fluorescence. The solution consisted of 1.1 μM MDCC−DTT adduct in 11 mM Tris·HCl (pH 8.0) at 20 °C with 0−90% ethanol. The solution at 100% ethanol was not buffered. Excitation was at 430 nm.

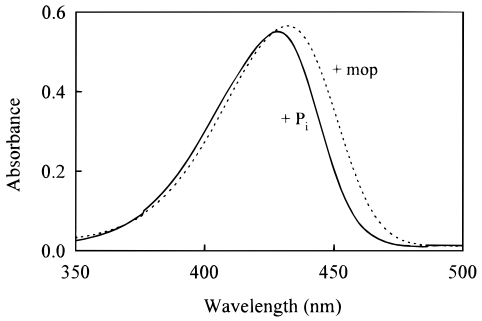

FIGURE 6: Absorbance spectra of MDCC−PBP in the presence and absence of P_i. The solution was 14 μM MDCC−PBP in 10 mM PIPES (pH 7.0) at 22 °C. P_i (35 μM) or the P_i mop (300 μM MEG and 1 unit mL^{-1} PNPase) was also present.

cence increases and there is a shift to a shorter wavelength for the emission maximum, similar to that observed for addition of P_i to MDCC−PBP. This suggests that such a change in environment could be a major cause of the fluorescence change of MDCC−PBP.

Fluorescence Quantum Yield. The absorbance spectrum of MDCC−PBP is dependent on P_i; there is a shift in the coumarin absorbance maximum on saturation with P_i, but the extinction coefficient changes only slightly (Figure 6). The quantum yield was measured for MDCC under several conditions as shown in Table 1. There is a 2−3-fold increase on attaching MDCC to the protein in the absence of P_i rather than to a small molecule, 2-mercaptoethanesulfonate, and a further 8-fold increase on binding P_i to MDCC−PBP. This

Table 1: Fluorescence Quantum Yields of Coumarins[a]

species	quantum yield
Coumarin 314 in ethanol	0.83[b]
Coumarin 314 in buffer	0.52
MDCC−2-mercaptoethanesulfonate adduct	0.014
MDCC−PBP, no P_i[c]	0.034
MDCC−PBP and P_i	0.27

[a] The measurements were taken in 50 mM HEPES (pH 7.0) at 20 °C. Emission spectra were obtained using solutions with absorbance of <0.05 and were then corrected for the photomultiplier profile and for baseline. Quantum yields were obtained by comparison with the values for Coumarin 314 in ethanol. [b] Literature value (*19*). [c] Treated with the enhanced P_i mop as in Figure 2.

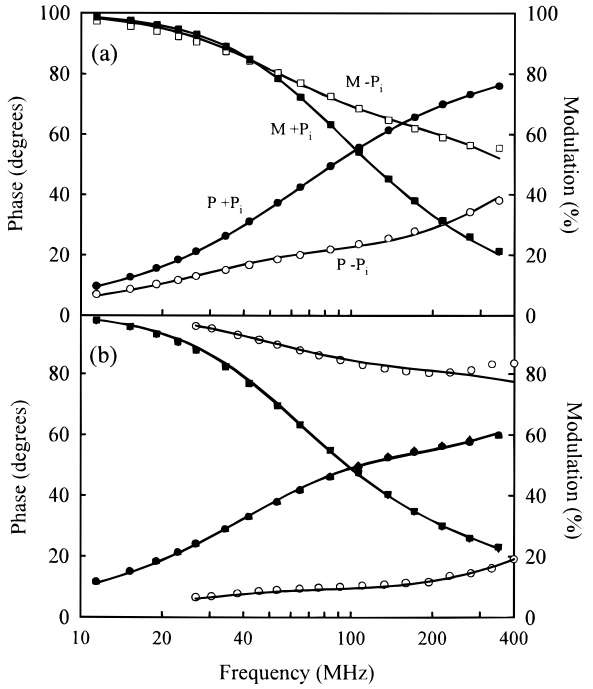

FIGURE 7: Multifrequency phase and modulation fluorescence data. (a) Responsive MDCC−PBP in the presence of the P_i mop (open symbols) or P_i (filled symbols). M = modulation, and P = phase. (b) MDCC−MES (open symbols) and MDCC−PBP S139C in the presence of the P_i mop or P_i (filled symbols). The best-fit lines are fit to two independent lifetimes, as given in Table 2. The solution conditions were 6 μM coumarin, 1.2 units mL^{-1} PNPase, and 375 μM MEG in 10 mM Tris·HCl (pH 7.5). P_i when present was added to 625 μM, leaving at least 250 μM free P_i after action of the P_i mop. The measurements were taken at 20 °C.

quantum yield is still 3-fold smaller than that of Coumarin 314 in ethanol. Note that the change in quantum yield does not correspond directly to the change in fluorescence intensity, as the latter is at a fixed wavelength (465 nm), and Figure 1 shows that there is a significant shift in the emission maximum when P_i binds to MDCC−PBP.

Fluorescence Lifetimes. Multifrequency phase and modulation data were obtained for the coumarin fluorophore in several environments (Figure 7) and were fit well by a double-exponential decay model (Table 2). The analyses indicated the presence of a short decay component with lifetimes of 0.2−0.6 ns and a second, longer decay component with lifetimes of 2.4−3.2 ns. The fractional contributions based on the intensity of the short lifetime components are given (Table 2) along with their relative molar fractions which were calculated using the assumption that the species lifetime is proportional to its quantum yield. When the

Table 2: Fluorescence Lifetimes of MDCC Coumarin in Various Environments[a]

sample[c]	lifetime (ns)		% of shorter lifetime[b] intensity	molar fraction	χ^2
MDCC−MES	0.19	3.06	82	99	1.0
MDCC−PBP without P_i	0.32	3.47	59	94	9.5
MDCC−PBP with P_i	0.70	2.38	5	14	0.6
nonresponsive without P_i	0.30	3.25	44	89	5.1
nonresponsive with P_i	0.36	2.41	42	83	4.7
S139C without P_i	0.40	3.24	17	62	3.8
S139C with P_i	0.39	3.19	16	62	5.1

[a] The experimental conditions are as in Figure 6. The values are from representative measurements, but for the responsive MDCC−PBP with P_i, four measurements, two each from two different protein preparations, were linked to fit a single pair of lifetimes, 2.35 and 0.47 ns, with an average χ^2 of 1.9. The data in the absence of P_i were more variable, probably because of variable, small amounts of remnant P_i; see the Discussion. The linked fit of four measurements gave values of 0.31 and 3.162 ns with an average χ^2 of 9.2. A χ^2 minimization map for the single measurements shown for the responsive MDCC−PBP gave the following ranges within a 67% confidence limit: without P_i, 57.3−61.1%, 0.301−0.336 ns, 3.22−3.76 ns; with P_i, 3.3−7.4%, 0.542−0.886 ns, 2.362−2.434 ns. [b] The percent of each lifetime component was calculated on the basis of fluorescence intensity fraction and converted to the molar fraction assuming the intensity is proportional to the lifetime. [c] "Nonresponsive" refers to the nonresponsive MDCC−PBP. "S139C" is this mutant PBP labeled with MDCC.

coumarin is attached to MES in solution, the lifetime of the coumarin is <0.2 ns, outside the range that can be measured accurately. There is also a small amount of fluorescence with a much longer lifetime (~3 ns). When the coumarin is attached to PBP, the data fit two lifetimes with one in the range of 0.2−0.6 ns and the other in the range of 2.3−3.5 ns in varying proportions depending on the state of the protein and coumarin. The percent of each lifetime, based on the fluorescence intensity, is converted to molarities assuming that the intensity of the coumarin fluorescence is proportional to the lifetime; i.e., quenching is dynamic.

In the absence of P_i, MDCC−PBP gives largely a short lifetime similar to that of the coumarin free in solution. The long lifetime component may be due in part to trace contamination by P_i. In the presence of P_i, the main component has a long lifetime (2.4 ns in the measurement shown), likely to be due to the closed conformation (MDCC−PBP*·P_i in eq 3). The short lifetime component (14%) can be ascribed in part to the small amount (3% by HPLC analysis) of the nonresponsive MDCC−PBP present which has mainly a short lifetime; albeit, the best fit is 0.36 ns for this and 0.70 ns for the responsive form. In addition, there may be some contribution by the open conformation which is in equilibrium with the closed form (eq 3) and might be expected to have a lifetime similar to that of the uncomplexed form; this will be discussed later.

The lifetimes of the nonresponsive protein do not change much on addition of P_i. The reduction in the longer lifetime from 3.2 to 2.4 ns by P_i may be consistent with the presence of a small percentage of responsive protein (3%). In the presence of P_i, this component is much more fluorescent than the nonresponsive protein and makes a major contribution to the longer lifetime intensity. The MDCC-labeled S139C PBP was measured as a control, because its fluorescence intensity is not changed by addition of P_i (*3*). Consistent with this, the lifetime measurements also show no change.

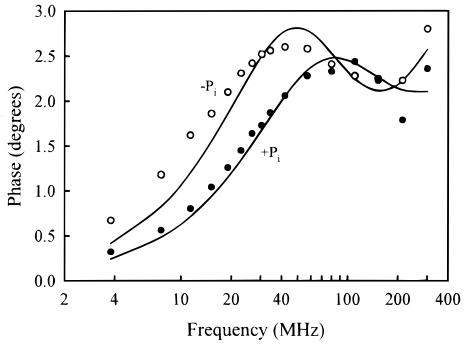

FIGURE 8: Multifrequency polarization phase data for MDCC−PBP in the presence and absence of P_i. The experimental conditions were as in Figure 7. The lines are best fit to these and modulation data (not shown) for two rotational correlation times, assuming limiting anisotropy is 0.4. Without P_i: 14.4 (79.5%) and 0.19 ns (20.5%), χ^2 (goodness of fit) = 4.1. With P_i: 28.0 (91.1%) and 0.13 ns (8.9%), χ^2 = 0.7. The nonresponsive MDCC−PBP gave the following values (data not shown): without P_i, 17.9 (82.2%) and 0.14 ns (17.8%), χ^2 = 1.9; with P_i, 15.2 (87.0%) and 0.10 ns (13.0%), χ^2 = 3.3.

Fluorescence Anisotropy. A shift in the steady state anisotropy, from 0.28 to 0.31, was observed with MDCC−PBP upon the addition of saturating concentrations of P_i. This result is consistent with either a change in the average rotational motion of the coumarin or, in the absence of a change in motion, a decrease in the intensity averaged fluorescence lifetime, τ_F ($\Sigma f_i \tau_i$, where f_i is the fractional intensity for the ith lifetime, τ_i). However, τ_F increases for MDCC−PBP from 1.6 (without P_i) to 2.3 ns (with P_i) and therefore cannot be the origin of the observed anisotropy increase. A restriction in rotational freedom of the coumarin probe due to P_i binding must be the source of the anisotropy change. To explore this issue, dynamic polarization data were collected for MDCC−PBP with or without P_i (Figure 8). The data fit well to a simple rotational model of a single species containing one slow rotational correlation time reflecting protein tumbling and one fast rotational correlation time reflecting the rapid probe motion at its point of attachment. The resolved slow rotational correlation time for the responsive MDCC−PBP in the absence of P_i was 14.9 ns (average of four measurements) which was found to increase significantly in the presence of P_i to 26.2 ns (average of six measurements). In contrast, the nonresponsive MDCC−PBP displayed little change in the slow rotational correlation time upon addition of saturating P_i (17.9 ns without P_i and 15.2 ns with P_i). The small percentage of the fast rotational correlation time (Figure 8) shows that there is little local tumbling.

Circular Dichroism. The CD spectra of the responsive and nonresponsive MDCC−PBP in the presence and absence of P_i were recorded as another probe of conformational changes (Figure 9). Far-UV CD spectra are derived from peptide bond absorbance and reflect protein secondary structure [reviewed by Woody (*20*)]. The spectra of the two forms of protein are identical and are not affected by P_i, showing that there is little change in secondary structure. The near-UV spectra (250−310 nm) are similar, suggesting little change in the tertiary structure affecting the environment of those aromatic residues that contribute to the near-UV signal. There are, however, large changes in the region of the coumarin absorbance. The coumarin chromophore itself

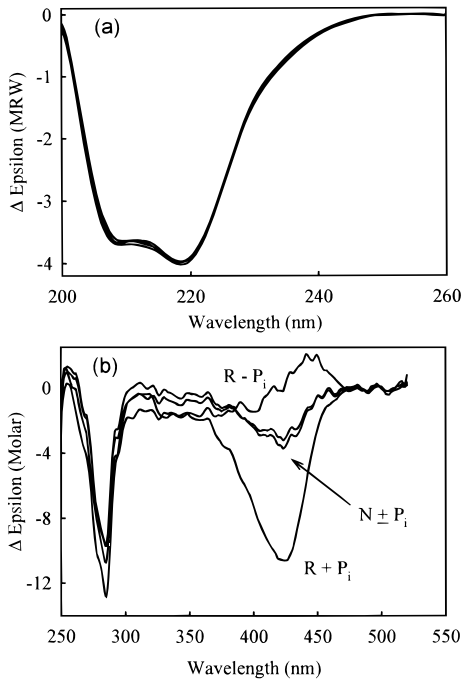

FIGURE 9: Circular dichroism spectra of MDCC−PBP. Spectra are for the responsive (R) and nonresponsive (N) proteins with (+) and without (−) P_i. The proteins were 10 mM PIPES (pH 7.0) at 4 μM (far-UV) and 20 μM (near-UV−visible, responsive) and 14 μM (near-UV−visible, nonresponsive). Proteins were previously treated with the P_i mop, and P_i was added to 100 μM. (a) Amino acid backbone absorbance region. (b) Coumarin and aromatic side chain regions. Multiple scans were averaged and baselines subtracted, and a small degree of numerical smoothing was applied. Spectra are presented as the circular dichroism absorbance coefficient calculated per residue (far-UV) and on a molar basis (near-UV−visible).

contains no chiral centers. The chiral center produced by the reaction of thiol with the maleimide (eq 2) is remote from the chromophore, so is unlikely to induce significant circular dichroism. Thus, any circular dichroism observed is most probably induced by the asymmetric protein environment. In the absence of P_i, the responsive MDCC−PBP shows only weak circular dichroism, suggesting that it is relatively mobile. Addition of P_i produces an intense negative peak at ~420 nm, suggesting that the coumarin becomes immobilized on the protein, consistent with the fluorescence data. In contrast, the nonresponsive MDCC−PBP has only a weak circular dichroism, with little change on binding P_i.

Sensitivity as a Phosphatase Activity Assay. Because of the increased purity of the MDCC−PBP, its sensitivity as a probe for P_i was assessed using a test reaction. The rate of D-glyceraldehyde-dependent ATPase activity of glycerokinase was measured using MDCC−PBP. Glycerokinase with D-glyceraldehyde specifically phosphorylates the aldehyde oxygen, so the product dissociates rapidly to glyceraldehyde and P_i (*21*). Figure 10 shows the fluorescence traces, with the ordinate converted to the amount of P_i; the observed rate is proportional to the amount of glycerokinase added. The signal-to-noise ratio of the traces is <2 pmol, and an accurate slope can be measured for 5 pmol of P_i released.

DISCUSSION

In applications of MDCC−PBP as a P_i probe for making real-time measurements of P_i release from phosphatases on a rapid time scale, both sensitivity and response linearity are important parameters. We have developed improvements in labeling and purification of this probe that double the signal increase on binding P_i over that previously reported. With the revised protocol, the probe appears to be a single species apart from the presence of diastereoisomers that current methods have not been able to separate.

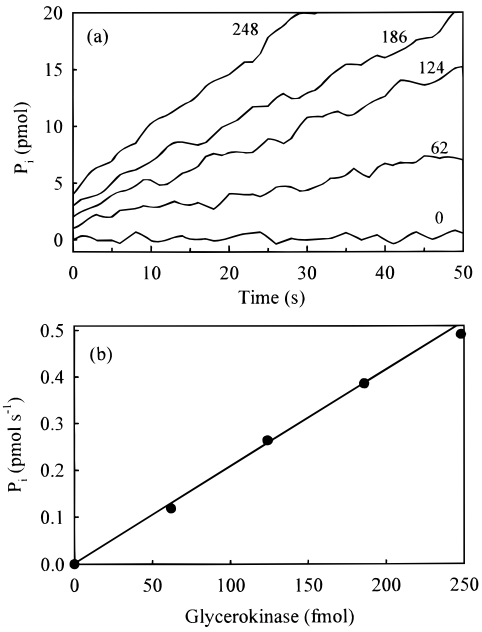

FIGURE 10: D-Glyceraldehyde-dependent ATPase activity of glycerokinase from *E. coli*, measured by MDCC−PBP fluorescence. The buffer at 25 °C with the enhanced P_i mop contained 20 mM Tris·HCl (pH 7.5), 1 mM $MgCl_2$, 40 μM $MnCl_2$, 0.7 μM glucose 1,6-bisphosphate, 136 μM 7-methylguanosine, 50 μg mL^{-1} PDRM, and 0.01 unit mL^{-1} PNPase. The assay solution contained in addition 1 μM MDCC−PBP and 100 μM ATP, and after the P_i mop was allowed to reduce P_i to a minimum (<0.05 μM in ~15 min), 1 mg mL^{-1} D-glyceraldehyde was added. (a) Aliquots (220 μL) of the assay solution were then put into fluorescence cuvettes (3 mm × 3 mm), previously treated for 10 min with the P_i mop, using the buffer as above. Aliquots of glycerokinase (<8 μL) were added to the assay solutions, and fluorescence was followed with time. Traces are offset by 1 pmol from each other at zero time for clarity. (b) The rate of P_i formation is proportional to glycerokinase concentration.

We have shown that MDCC−PBP is susceptible to base-catalyzed hydrolysis and suggest that this is at the succinimide ring as in eq 1, but such hydrolysis is not significant during preparation and purification of MDCC−PBP. Base-catalyzed hydrolysis of maleimide−cysteine adducts has been demonstrated previously (*22*, *23*). There is no sign of a rearrangement of the succinimide by reaction with a protein amine, as described previously (*24*−*26*); this would have been detected as an extra peak in the peptide digest pattern. A small amount of labeling occurs on a second site (probably K175), but this doubly labeled species is negligible under the revised conditions.

The use of consecutive chromatographic steps in the absence and then in the presence of P_i has allowed removal of a component of MDCC−PBP, whose fluorescence does not respond to P_i. This species has exactly the same mass and tryptic digest pattern as the P_i-responsive probe. The amount of this second species varies between preparations, and a long incubation of the P_i-sensitive MDCC−PBP results in a small amount of a product that has the same ion

exchange properties as the P_i-insensitive MDCC−PBP. This suggests a rearrangement that does not change the mass, but currently there is no evidence for the nature of this change, whether to protein or label or the interaction between the two. The circular dichroism measurements suggest that there are unlikely to be gross changes to the protein secondary structure, such as partial unfolding. Several lines of evidence indicate that the nonresponsive protein binds P_i, although giving little or no fluorescence change. First, its elution position on ion exchange chromatography changes with added P_i. Second, an excess of this protein can remove P_i from the responsive MDCC−PBP, in the same way as the wild type protein. Third, the kinetics of P_i release from the nonresponsive protein could be measured, albeit giving a rate 10-fold faster than that of the responsive MDCC−PBP. This nonresponsive form has spectroscopic properties that suggest an open conformation in the coumarin region, with the coumarin in an environment like the P_i-free responsive form.

In all the kinetic and spectroscopic analysis, it has not been possible to differentiate between the diastereoisomers. The major evidence for their presence comes from the tryptic digest analysis and from the crystal structure (*8*). Evidence that both isomers bind P_i with a fluorescence change comes directly from the fluorescence titration (Figure 2). Consider that, if only 50% of the protein were active, then the break in the curve would be at 2.8 μM in the data shown (50% of the protein concentration). In fact, the increase in fluorescence is still approximately linear at this concentration, and the break is at 70−80%, in the many titration curves done with different preparations of this protein. Although the titration curve alone could not be fitted to give precise values of fluorescence change and K_d for each isomer, one isomer [assumed to be *R*-configuration at the succinimide on the basis of the crystal structure (*8*)] binds P_i tighter with a several-fold larger fluorescence change. In principle, a simpler model is possible in which only the tighter binding isomer produces a fluorescence change, but this does not fit the titration data as well. In addition, the fluorescence lifetime data (Table 2) suggest that most of the protein has an increased lifetime on binding P_i. In any case, all the fluorescence measurements (kinetic and time-resolved) will be dominated by the properties of the *R*-isomer. These data are mainly discussed in terms of one population of protein, but we also discuss how they might be reconciled with the presence of two diastereoisomers.

The crystal structures of PBP reported for the P_i-bound (*27*) and P_i-free forms (*18*) show that there is a large hinge-bending motion between the two structures producing a large cleft in the absence of ligand. The kinetic and spectroscopic data with MDCC−PBP suggest that, in the absence of P_i, the protein cleft is open and the coumarin is in a hydrophilic environment. P_i binding causes cleft closure with a concomitant increase in the hydrophobicity around the coumarin and hence the changes in fluorescence and circular dichroism. From the anisotropy data, there is a decrease in mobility, as shown by the fractional amount of the local (rapid) motion. The change in the rate of reaction of the A197C thiol with DTNB by almost 2 orders of magnitude is consistent with such cleft closure. We will now discuss how the kinetic and spectroscopic data are consistent with these ideas.

Both the kinetic and spectroscopic data can be explained in terms of the two-step binding model in eq 3, although there are insufficient rate data to obtain a unique set of rate constants for this scheme. The saturating rate of 322 s^{-1} at 5 °C corresponds to $k_2 + k_{-2}$. The DTNB−thiol reaction kinetics can be used to estimate the equilibrium between open and closed conformations, assuming that only the open conformation reacts with DTNB. This is a reasonable assumption, on the basis of an examination of the crystal structure of the P_i-bound A197C mutant protein that shows the thiol is buried (*8*). The 70-fold decrease in the rate on addition of P_i (at 20 °C rather than at 5 °C, although a similar ratio was obtained at 12 °C) would mean that there is 1.4% open conformation at equilibrium. This in turn suggests that k_2 is 317 s^{-1} and k_{-2} is 4.5 s^{-1}, close to the value of the dissociation rate constant of P_i measured from MDCC−PBP (4.8 s^{-1}).

This dissociation rate corresponds to $k_{-1}k_{-2}/(k_2 + k_{-1})$, so this function is approximately equal to k_{-2}, $k_{-1} \gg k_2$. This in turn justifies fitting the P_i dependence of the binding kinetics (Figure 3) to give a value of 4.9 μM for $1/K_1$. So K_d ($k_{-1}k_{-2}/k_1k_2$) is 0.07 μM, close to that suggested by an equilibrium titration (*3*). If k_{-1} is >1500 s^{-1} ($5k_2$), then k_1 is $>3.8 \times 10^8$ M^{-1} s^{-1} and so probably diffusion-controlled. The reversibility of the reaction is presumably important for the normal biological function of PBP; in vivo, the periplasmic PBP, after "capturing" P_i, must release it to a membrane protein for import into the cytoplasm.

P_i dissociation kinetics are apparently constant for different levels of saturation, suggesting k_{-2} is the same for each diastereoisomer. However, it is unlikely that the binding kinetic measurements could resolve two components, one with probably <25% the intensity change of the other at saturating P_i concentrations (Figure 2). This relative intensity will decrease at lower P_i concentrations when one isomer is not saturating. At high P_i concentrations, the rates are very fast even at 5 °C, so most of the signal is lost in the dead time of the stopped flow instrument. So we assume that the rate constants obtained are close to those of the *R*-isomer.

The fast and slow rotational correlation times are commonly interpreted as the local probe motion and the slow tumbling of the protein, respectively. The Stokes−Einstein relationship can be used to predict a rotational correlation time for the protein based on rotation of a spherical body:

$$\tau_c = \frac{M(\nu + \delta)\eta}{RT} \qquad (4)$$

where τ_c is the rotational correlational time, M is the molecular weight, ν is the specific volume of the protein, δ is the hydration specific volume, η is the viscosity, R is the gas constant, and T is the temperature. The analytical ultracentrifugation data show that MDCC−PBP is a monomer. At 20 °C, δ is 0.4 cm^3 g^{-1} and ν is 0.73 cm^3 g^{-1}, giving an estimate of 16.3 ns for the PBP rotational correlation time. Given the potential errors in the assumptions, this theoretical estimate agrees well with the recovered values for P_i-responsive MDCC−PBP (without P_i) and the nonresponsive MDCC−PBP (with or without P_i) which range from 15 to 18 ns. However, on P_i binding, the former shows a significant increase in the long rotational correlation time to 26.2 ns (average). An increase can be explained by a change in the relative orientation of the probe to the rotational axes of an asymmetric protein together with the large

conformational change on P_i binding. MDCC−PBP•P_i has an asymmetric shape approximating a prolate ellipsoid with an axial ratio of 2:1 with the angle between the coumarin and the protein long axis being 30−45° (*8*), depending on how the structure is fitted to the symmetrical model and how the transition dipole of the coumarin is defined. On the basis of the lower angle, a single rotational correlation time of 22 ns can be calculated (*28*). Given the precision of the data and the simplifications inherent in the model, the values from experiment and theory seem to be consistent with each other. This indicates a dramatic change in the coumarin orientation upon P_i binding, and this point will be discussed further in relation to the crystal structure (*8*).

The CD spectra show that there are no overall changes in the α-helical content on P_i binding. In the coumarin absorbance region, the changes in the responsive form on P_i binding are consistent with the open and closed conformations model. In the absence of P_i, the signal is small but non-zero, so the coumarin is not as in free solution but has a weakly asymmetric environment derived from the surrounding protein structure, consistent with the fluorescence data.

The multiple fluorescence lifetimes of the responsive MDCC−PBP can be rationalized in terms of multiple protein species. In the absence of P_i, the lifetime is short, but a small amount of P_i could explain the long component. In the presence of P_i, the small amount of short lifetime component will include contributions from the nonresponsive impurity and probably from the open conformational state of MDCC−PBP•P_i in equilibrium with the closed state. The observed 13-fold increase in fluorescence intensity and 8-fold increase in quantum yield are consistent with the changes in the fluorescence lifetimes, so any quenching effects are likely to be dynamic.

The fluorescence lifetime data were fit to a model with two time constants; the degree of accuracy of the data does not justify fitting an additional, minor component to account for the difference between the diastereoisomers. The lifetime overlap between the two isomers is too close to resolve accurately the two species by fluorescence lifetime measurements.

Our previous data (*3*) showed that minor changes to the structure of MDCC, e.g., changing the spacer length between maleimide and coumarin from two carbons to three or changing to an iodoacetamide of the same chain length as in MDCC, have a large effect on the P_i-induced fluorescence change, so it is likely that the coumarin in MDCC−PBP needs to be precisely positioned for the changes described above. This precise need is explained well by the crystal structure in the following paper (*8*).

The MDCC−PBP prepared using the methods described here shows a 13-fold increase in fluorescence on P_i binding, the improvement compared to our previous data (*3*) being achieved by use of the enhanced mop, both during labeling and for providing P_i-free MDCC−PBP, and by further chromatography. Although the titration with P_i (Figure 2) is consistent with a single population of ∼75% active protein (*3*), it seems more likely that the two diastereoisomers differ in K_d and P_i-induced fluorescence change. The titration can then be described by two phases, linear to 50% saturation, representing mainly tight binding to one diastereoisomer, followed by a curve to 100% saturation as the other, weaker binding diastereoisomer becomes saturated. It is therefore prudent to use this probe up to 50% saturation for the most accurate work, although in practice the titration is linear to ∼70% saturation. The kinetic data are consistent with this model, but it does not seem that the spectroscopic properties at zero or saturating P_i concentrations can differentiate between the diastereoisomers in the 50:50 mixture.

The sensitivity of MDCC−PBP as an assay of phosphatase activity was tested in a reaction in which formation of nanomolar amounts of P_i was measured. Use of the P_i mop allowing the P_i background to be reduced to low levels and the continuous monitoring of fluorescence minimize the problems due to P_i contamination. Other nonradioactive methods are limited by this contamination, and so for many uses, MDCC−PBP will be more sensitive than, for example, the phosphomolybdate methods based on the procedure of Fiske and SubbaRow (*29*). Such methods cannot be used in situ and require a separate incubation for each assay, so the sensitivity and ability to monitor P_i continuously are considerable advantages of MDCC−PBP for many applications.

In conclusion, we have used the coumarin-labeled PBP to characterize the two-step P_i binding mechanism and have obtained a kinetic scheme that satisfies the available data for the rates of interconversion and equilibrium constants between states. The concomitant change to the coumarin to produce a high-fluorescence state has also been probed. The relationship between these changes is discussed further by Hirshberg et al. (*8*), where the crystal structure of the MDCC−PBP provides an atomic resolution description of the environment of the coumarin.

ACKNOWLEDGMENT

We thank Dr. John Eccleston (NIMR, London) for making the analytical ultracentrifugation measurements.

REFERENCES

1. Quiocho, F. A. (1991) *Curr. Opin. Struct. Biol. 1*, 922−933.
2. Mao, B., Pear, M. R., McCammon, J. A., and Quiocho, F. A. (1982) *J. Biol. Chem. 257*, 1131−1133.
3. Brune, M., Hunter, J. L., Corrie, J. E. T., and Webb, M. R. (1994) *Biochemistry 33*, 8262−8271.
4. Gilbert, S. P., Webb, M. R., Brune, M., and Johnson, K. A. (1995) *Nature 373*, 671−676.
5. He, Z. H., Chillingworth, R. K., Brune, M., Corrie, J. E. T., Trentham, D. R., Webb, M. R., and Ferenczi, M. A. (1997) *J. Physiol. 501*, 125−148.
6. Lionne, C., Brune, M., Webb, M. R., Travers, F., and Barman, T. (1995) *FEBS Lett. 364*, 59−62.
7. Nixon, A. E., Brune, M., Lowe, P. N., and Webb, M. R. (1995) *Biochemistry 34*, 15592−15598.
8. Hirshberg, M., Henrick, K., Lloyd Haire, L., Vasisht, N., Brune, M., Corrie, J. E. T., and Webb, M. R. (1998) *Biochemistry 37*, 10381−10385.
9. Willsky, G. R., and Malamy, M. H. (1976) *J. Bacteriol. 127*, 595−609.
10. Gill, S. C., and von Hippel, P. H. (1989) *Anal. Biochem. 182*, 319−326.
11. Corrie, J. E. T. (1994) *J. Chem. Soc., Perkin Trans. 1*, 2975−2982.
12. Aitken, A., Howell, S., Jones, D., Madrazo, J., and Patel, Y. (1995) *J. Biol. Chem. 270*, 5706−5709.
13. Spencer, R. D., and Weber, G. (1970) *J. Chem. Phys. 52*, 1654−1663.
14. Gratton, E., and Limkeman, M. (1983) *Biophys. J. 44*, 315−324.

15. Gratton, E., Jameson, D. M., and Hall, R. D. (1984) *Annu. Rev. Biophys. Bioeng. 13*, 105−124.
16. Jameson, D. M., Gratton, E., and Hall, R. D. (1984) *Appl. Spectrosc. Rev. 20*, 55−106.
17. Spencer, R. D., and Weber, G. (1969) *Ann. N.Y. Acad. Sci. 158*, 361−376.
18. Ledvina, P. S., Yao, N., Choudray, A., and Quiocho, F. A. (1996) *Proc. Natl. Acad. Sci. U.S.A. 93*, 6786−6791.
19. Fletcher, A. N., and Bliss, D. E. (1978) *Appl. Phys. 16*, 289−295.
20. Woody, R. W. (1995) *Methods Enzymol. 246*, 34−71.
21. Hayashi, S., and Lin, E. C. C. (1967) *J. Biol. Chem. 242*, 1030−1035.
22. Knight, P. (1979) *Biochem. J. 179*, 191−197.
23. Ishii, Y., and Lehrer, S. S. (1986) *Biophys. J. 50*, 75−80.
24. Smyth, D. G., Nagamatsu, A., and Fruton, J. S. (1960) *J. Am. Chem. Soc. 82*, 4600−4604.
25. Witter, A., and Tuppy, H. (1960) *Biochim. Biophys. Acta 45*, 429−442.
26. Wu, C.-W., Yarbrough, L. R., and Wu, F. Y. (1976) *Biochemistry 15*, 2863−2868.
27. Luecke, H., and Quiocho, F. A. (1990) *Nature 347*, 402−406.
28. Beechem, J. M., Knutson, J. R., and Brand, L. (1986) *Biochem. Soc. Trans. 14*, 832−835.
29. Fiske, C. H., and SubbaRow, Y. (1925) *J. Biol. Chem. 66*, 375−400.

BI9804277